ADVANCED SENSOR RESEARCH Open Access
www.advsensorres.com

Modular Multi-Parametric and Portable Readout System for Point-of-Care Applications

*Dibyendu Khan, Thossaporn Wijakmatee, Aniruddha Sriram, Aidin Nikookhesal, Elmar Weinhold, Yusuke Shimoyama, Vivek Pachauri, and Sven Ingebrandt**

A portable, battery-powered, multi-purpose readout system for combined optical and thermal measurements is presented. The system is modular with four independent input channels for different measurement schemes, allowing simultaneous multi-parameter measurements to detect analytes of interest. Combined optical and thermal readout for spectroscopy is implemented by installing two different analog front-end modules in the four input channels equipped with a micro spectrometer and a high-resolution temperature sensor, respectively. The readout system is utilized to measure fluorescence signals of a common dye functionalized on gold nanoparticle-DNA conjugates as a function of the temperature. Gold nanoparticles are modified with Guanine-rich DNA sequences to perform Förster Resonance Energy Transfer (FRET) measurements. Elongation of DNA sequences at higher temperatures resulted in stronger fluorescence signals, accurately recorded by the portable system. The precision electronic components are chosen for a precise, battery-powered operation. The size of this versatile, compact, and portable instrument is only 15.6 × 10.6 cm^2. An interactive graphical-user-interface developed for this system supports point-of-care usage. The measurements carried out with the portable system showed a very close match with a commercial set-up, with deviations less than 1 nm in the optical spectra and less than 0.5 °C in temperature.

1. Introduction

Spectroscopic and colorimetric measurement techniques like fluorescence spectroscopy and optical microscopy for enzyme-linked immunosorbent assays, Bradford assays etc., are routinely used because of their high accuracy and sensitivity.[1,2] Such fluorescence or color-based assays are utilized in different application fields such as in pharmaceutical industry, biomedical diagnostics and environmental monitoring. Depending on the transduction principle and measurement method, the optical signal needs to be measured in a static or dynamic manner. In the static case, recording a pH-related color change in the visible light spectrum and related intensity measurements give an end-point analysis of fast chemical reactions. Dynamic recording of optical signals are advantageous to monitor slow but complex processes in biological systems. There the use of fluorescent dyes is widespread in order to characterize biomolecular interactions, e.g., antigen-antibody assays, DNA hybridization assays, as well as changes in molecular conformations.[2–4] High accuracy optical measurements typically need precise desktop spectrometers that facilitate high-quality light sources and bulky optical components. Such analytical equipment can facilitate multiple measurement points to achieve a high sample throughput in semi- or fully-automated laboratory workflows, but need a controlled laboratory environment for biomedical diagnostics or analytical chemistry.

D. Khan, A. Nikookhesal, V. Pachauri, S. Ingebrandt
Institute of Materials in Electrical Engineering 1
RWTH Aachen University
Sommerfeldstraße 24, 52074 Aachen, Germany
E-mail: ingebrandt@iwe1.rwth-aachen.de

The ORCID identification number(s) for the author(s) of this article can be found under https://doi.org/10.1002/adsr.202400105

DOI: 10.1002/adsr.202400105

T. Wijakmatee, Y. Shimoyama
Department of Chemical Science and Engineering
Tokyo Institute of Technology
2-12-1 S1-33, Ookayama, Meguro-ku, Tokyo 152–8550, Japan

A. Sriram
Department of Electrical Engineering
Indian Institute of Technology Madras
Chennai 600036, India

E. Weinhold
Institute of Organic Chemistry
RWTH Aachen University
Landoltweg 1, 52056 Aachen, Germany

In some niche applications such as agricultural and environmental monitoring, there is a high demand for manual, on-site sensor measurements or even for the integration of sensor-networks for an automated real-time analysis of target analytes.[5] Main attributes of such on-site measurement scenarios, in addition to an accurate readout, are cost-effectiveness and portability. Thereby, selection of suitable miniaturized components and innovative integration concepts are highly sought-after for the optimization of measurement sensitivity and signal reliability. The possibility to acquire multiple signals in parallel is needed for stable response in measurement scenarios outside of the controlled laboratory environment. For point-of-care readout systems, a significant improvement is expected by implementing a multiple parameter readout, which allows monitoring and controlling of influencing side parameters (e.g., temperature, pH value, and ionic strength of the test solution). Combining related but independent transducer principles is highly beneficial for the detection of analytes with high accuracy. By utilizing combinatorial signal analysis, the miniaturized portable sensor systems might complement laboratory-based analysis and in certain applications (e.g., biomedical, agriculture, and environmental monitoring) provide a serious alternative as distributed sensor networks.

The integration of readout tools that combine precise optical and thermal monitoring is essential for many chemical and biological assays.[6] For example, fluorophores like Rhodamine B,[7] calcium-sensitive fluorescent probes like Fura-2, Indo-1, Quin-2,[8] have a temperature dependent spectral output. The surrounding temperature influences the overall efficiency of the molecular binding interactions, enzymatic conversion, and DNA hybridization. Recording of temperature over time would be beneficial in such assays as well.[6,9] Several nanomaterials such as nanoparticles and quantum dots, which are often used to enhance the signal output, exhibit temperature-dependent optical characteristics. Therefore it can be stated, that the parallel recording of temperature and optical spectra is essential to carry out an accurate analysis in many applications.[10]

Amongst nanoparticles, colloidal gold nanoparticles (AuNPs) are widely used as colorimetric sensors for the detection of different analytes.[11–13] AuNPs-DNA conjugates have been used for the detection of a wide variety of molecules like cocaine,[14] potassium ions,[15] lead ions,[16,17] etc. Thereby, the specific binding of an analyte at the nanoparticle (NP) surface changes the morphology or the conformation of the biomolecules (DNAs, aptamers, proteins etc.). When utilizing a fluorescence-based detection, the fluorescence intensity changes based on the proximity of the fluorophore dye to its quencher, i.e., a metallic surface or a metallic NP.[18] In case of colorimetric detection, a change in color will occur due to the aggregation of the NPs triggered by morphological or conformational changes of for instance an aptamer.[12] One example of such secondary DNA structures, a guanine-rich nucleosequence, was described as a promising target for cancer therapy.[19,20] Guanine-rich sequences are known to undergo large conformational changes induced by temperature.[21] Förster Resonance Energy Transfer (FRET) based assays utilizing temperature dependent folding and unfolding of DNA sequences has been characterized by other researchers using conventional laboratory-based set-ups.[22–24]

We report the development of a portable readout system that can be used for highly sensitive optical and thermal measurements in parallel (**Figure 1**). The compact system with dimensions of only 15.6 cm × 10.6 cm fits the requirements of a battery-powered, portable set-up for hand-held, on-site deployment in real-time applications. To the best of our knowledge, such modular multi-parametric and portable readout system for point-of-care applications has not been reported so far. To prove its utility and to combine its thermal and optical functionalities in an exemplary biosensor assay, we investigated the unfolding mechanism of two guanine-rich DNA sequences as a function of temperature. The guanine-rich DNA was tagged with a red fluorescence dye (Atto 633, Sigma–Aldrich, Germany) and tethered onto AuNPs of ≈13 nm diameter.

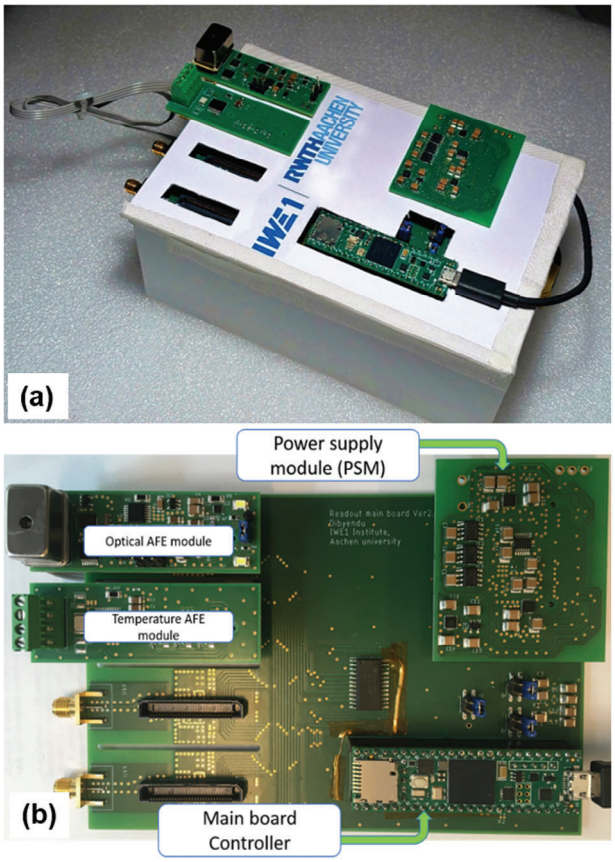

Figure 1. a) Portable, battery-powered four-channel readout system with a single board minicomputer for combined optical and thermal measurements. b) Different components of the portable, battery-powered four-channel readout system for combined optical and thermal measurements are shown. On the left side, two of the four channels are equipped with specialized analog front-end (AFE) modules. The measured data can be logged onto an SD card, transferred via the USB port, or transmitted wirelessly.

At lower temperatures, the guanine-rich DNA sequences remain folded keeping the fluorophores close to the AuNPs surface leading to a quenching of the fluorescence based on the Förster Resonance Energy Transfer (FRET) mechanism. When the temperature is increased, the guanine-guanine interactions are weakened and the sequences start to unfold resulting in an elongation of the nucleic acid backbone pushing the fluorophores away from the AuNPs surface. This leads to a temperature-dependent

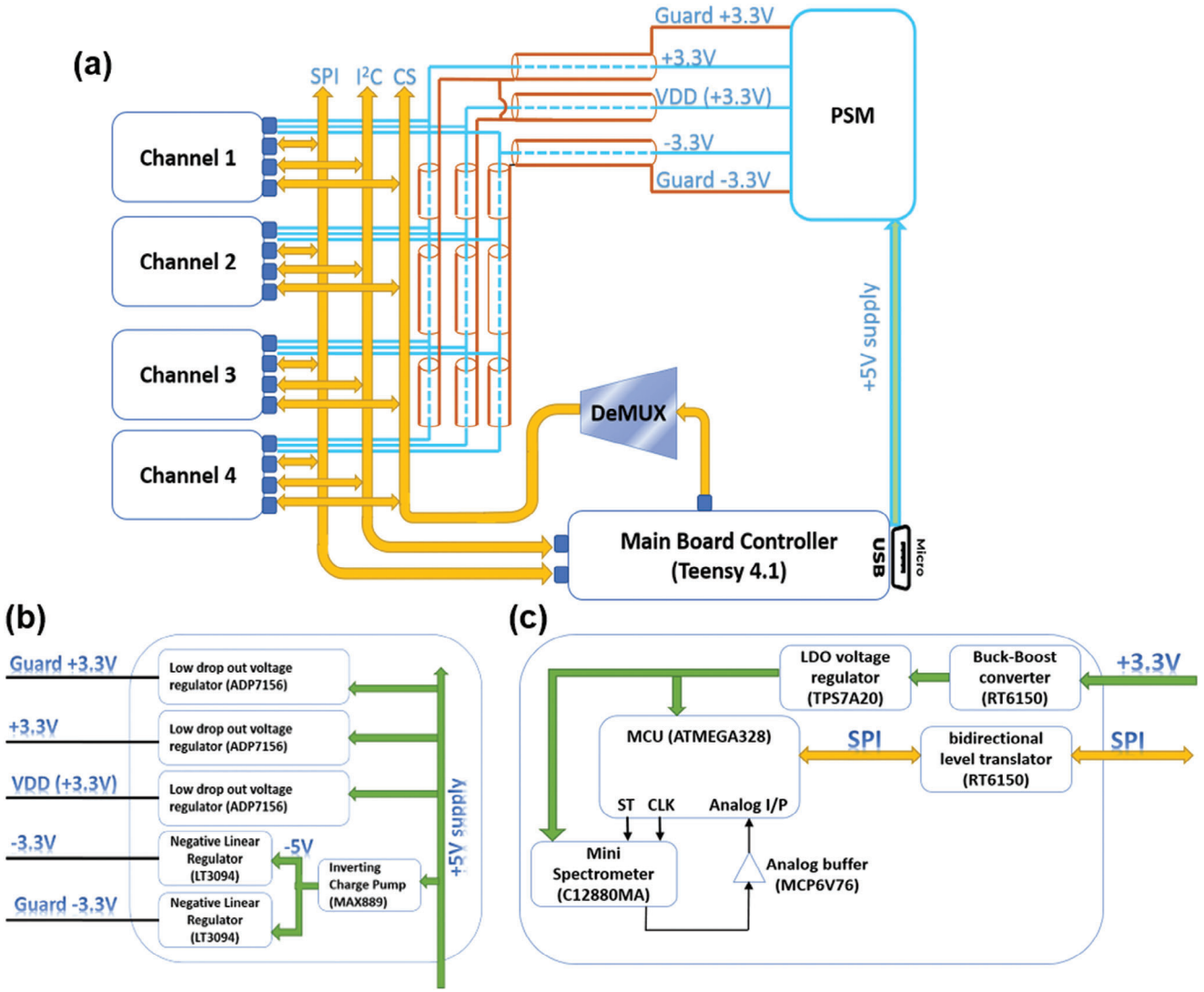

Figure 2. Schematics of a) the main board of the readout system. Four channels are connected by SPI and I^2C communication to the main board controller. A de-multiplexer (DeMUX) allows for chip select (CS). The power supply module (PSM) supplies the voltages, while in b) inverting charge pumping is used to generate the 5 V supply for the mini spectrometer. The optical AFE module shown in c) consists of the ATMEGA328 MCU and the mini spectrometer module C12880MA.

fluorescence recovery, which can be detected by the mini spectrometer of the system using a suitable filter in front of its optical input. We chose this assay as a proof-of-concept in order to display the system's in-parallel measurement functionality. The practical usage of the system, however, is generic since many bio- or chemosensor assays such as sandwich, competitive binding or other could be easily implemented.

2. Experimental Section

The multi-parametric readout system has a modular concept and is made of four different instrument modules, including a main board, a power supply module (PSM), an optical analog front end (AFE), and a temperature sensor AFE (Figure 1b). This concept allowed for independent development and optimization of the different AFE modules. It also ensures an easy upgrade for future incorporation of additional measurement functionalities. As shown in Figure 1a, the portable system utilizes a minicomputer (LattePanda3Delta,[25] Mouser Electronics, Germany) (LattePanda) and a generic power bank to power the whole system. In operation, the LattePanda was connected to a WiFi network and the readout system can be fully controlled from a remote location through a remote server. In the following, the key characteristics of the different modules were discussed and provide a detailed discussion on their on-board integration to realize the multi-parametric sensor system.

2.1. Main Board and the Power Supply Module

The main board has an open-ended design allowing future upgrades with other specialized AFE modules. The board consists

Table 1. Two derivatives of a guanine-rich DNA sequences labeled with the Atto633 fluorophore dye.

QP-DNA1	5Atto633/TGTGTAGTGTGTGGAGTGTGTGGAAGGAAAAAAAAAA/3ThioMC3-D
QP-DNA2	5Atto633/TGAGGGTGGGTAGGGTGGGTGTGAGTGAAAAAAAAA/3ThioMC3-D

of the power supply module (PSM), the main board controller (Teensy 4.1 development board from PJRC.COM, Reichelt Elektronik, Germany), and four independent channels with I^2C and serial peripheral interface (SPI) communication. In the current layout, two of these channels were equipped with one optical and one thermal AFE module, while the two remaining channels allow a future expansion of the readout system. The board was powered with 5 V supply from the universal serial bus (USB) port of the Teensy 4.1 development board. The PSM managed the 5 V supply to create the operating (VDD) and the guard voltage (Guard) of 3.3 V, respectively, which are required for the operation of the AFE modules.

The PSM consisted of three low noise, low drop out (LDO) voltage regulators (ADP7156ACPZ-3.3-R7 Analog Devices Inc., USA) for the analog and digital supply as well as for the positive guard signaling. The PMS module utilized an inverting charge pump (MAX889 from Analog Devices Inc., USA) and two low noise negative linear regulators (LT3094 from Analog Devices Inc., USA) to also create −3.3 V and the negative guard signal, respectively. The analog ground and the digital ground of the entire board were separated, and star connected closely to the supply point. Each of the four AFE channels were connected with four active low chip select (CS) signals for communication with four independent devices. The CS signals were generated with a high-speed silicon gate and a 4 to 16 line decoder/de-multiplexer (DeMUX) (CD74HC4515M from Texas Instruments Inc., USA). The four inputs of the decoder/de-multiplexer come directly from the Teensy 4.1 main board controller. The schematic illustration of the main board and the PSM are shown in **Figure** 2a,b.

2.2. Optical Analog Front End

The optical AFE utilizes a highly sensitive mini spectrometer (C12880MA from Hamamatsu Photonics K.K., Japan) and a low power microcontroller (MCU) (ATMEGA328 from Microchip Technology Inc., USA) to control the optical AFE module and to communicate with the main board controller. The mini spectrometer in fingertip size (20.1 × 12.5 × 10.1 mm) exhibits a spectral response range of 340–850 nm with a maximum spectral resolution of 15 nm and operates at 5 V. Since the operating voltages of the main board and the main board controller (Teensy 4.1) are 3.3 V, respectively, the voltage supply of the spectrometer needs to be boosted to 5 V using a buck-boost converter (RT6150 from Richtek Inc., USA) and an LDO voltage regulator (TPS7A20 from Texas Instruments Inc., USA). The output of the spectrometer was an analog signal, which feeds through an analog buffer (MCP6V76 from Microchip Technology Inc. USA) to the analog-to-digital converter (ADC) input of the ATMEGA328 MCU. The SPI communication between the ATMEGA328 MCU and the main board controller was realized by a bi-directional level translator (TXB0104-Q1 from Texas Instruments Inc., USA). The clock (CLK) and the start pulse (ST) for the ATMEGA328 MCU provide the operational control of the mini spectrometer. For recording of the optical spectrum, the ATMEGA328 MCU receives instructions from the main board controller, then issues appropriate CLK and ST signals to the spectrometer, which internally reads the optical spectrum and sends it back to the ATMEGA328 MCU. The MCU is operated at 16 MHz and its ADC has a resolution of 10bits. The data is stored in the ATMEGA328 MCU and sent back to the main board controller on request. This on-request data management allows freeing up the main board during recording ensuring parallel measurement with all channels. The schematics of the optical AFE module is shown in Figure 2c. The correlation between pixel number and wavelength can be derived from a fifth order polynomial Equation (1) provided by the manufacturer for the calibration of each spectrometer. The coefficients of the polynomial equation for the spectrometer with serial number 22C05035 are as follows:

$$Wavelength\ [nm] = A_0 + B_1 * x + B_2 * x^2 + B_3 * x^3 + B_4 * x^4 + B_5 * x^5 \quad (1)$$

with x = Pixel number, A_0 = 312.202703067139, B_1 = 2.72150451113498, B_2 = − 0.00141709209942523, B_3 = − 6.02341430640447*10^{-6}, B_4 = 4.2868806388869*10^{-9}, B_5 = 1.08635798172687*10^{-11}

2.3. Temperature Sensor AFE Module

The temperature sensor AFE module consists of a resistive temperature detector (RTD) (PT1000 class A, Reichelt Elektronik, Germany) having range from −30 to +300 °C and a resistance-to-digital converter (MAX31865 from Maxim Integrated, USA). A resistor reference (R_{ref}) of 4020 Ohm and an SPI mode 3 communication is used to communicate with the main board controller. The MAX31865 includes a 15 bit resolution ADC, which can be used to calculate the resistance of the PT1000 (R_{PT1000}) as shown in Equation (2):

$$R_{PT1000} = \frac{(ADC\ output * R_{ref})}{2^{15}} \quad (2)$$

The temperature can be calculated by using the Callendar–Van Dusen Equation (3):

$$R_{PT1000} = R_0 \left(1 + a*T + b*T^2 + c\,(T - 100)\,T^3\right) \quad (3)$$

Here, the coefficients for this polynomial equation are: a = 3.90830*10^{-3}, b = −5.77500* 10^{-7}, and c = −4.18301*10^{-12} for −200 °C ≤ T ≤ 0 °C and 0 for 0 °C ≤ T

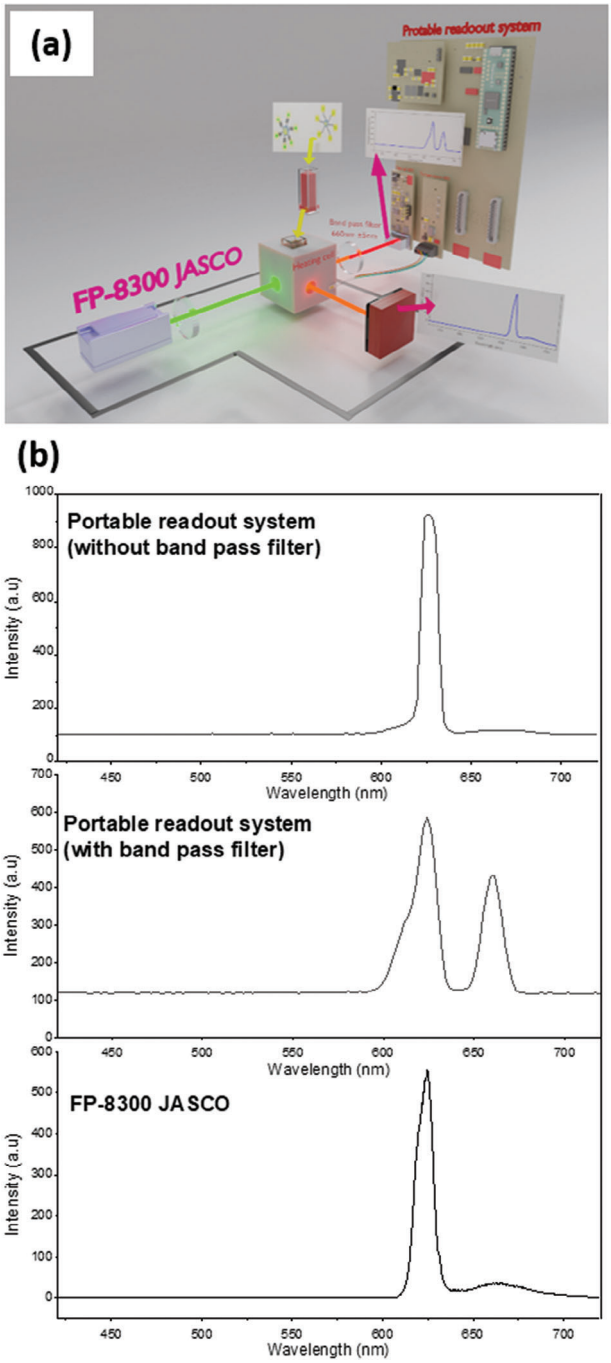

Figure 3. a) Measurement scheme used for the characterization of the DNA-AuNP conjugates at room temperature including the newly developed portable, multi-parametric readout system. b) Top and middle: Optical spectrum recorded with the portable readout system using the light source of a Jasco FP-8300 spectrometer without and with an optical filter. Bottom: Optical spectrum recorded only with the desktop spectrometer. The peat at 625 nm is the excitation wavelength and the peat at 657 nm shows the fluorescence intensity in arbitrary units (a.u.). The excitation peak recorded with the portable instrument (b middle) is significantly suppressed by the optical filter in the light path changing the ratio between the two peaks. The y-axis displays arbitrary units after internal amplification, respectively.

2.4. DNA Sequences for the FRET-Based Assay

The guanine-rich DNA sequences that were investigated for the FRET based assay are shown in **Table 1**. Both sequences are derived from the human genomic sequence Pu27, while six guanines bases are replaced with thymine, whereas for Mcy22 the outermost G-track of Pu 27 was removed and one guanine base from each of the two G-tracks containing four guanine bases is replaced with a thymine base.[26,27] Last, both Pu27 6G/T and Mcy22 AuNP-DNA conjugate sequences were extended to the original length of 37 nucleotides (nt) by adding additional Adenosine bases.

2.5. Synthesis of the AuNP-DNA Conjugates

2.5.1. Materials

Deionized water was prepared using a Milli-Q Type 1 ultrapure water system from Merck KGaA, Germany. Gold(III) chloride ($AuCl_3$, purity >99.0%) and monobasic potassium phosphate (KH_2PO_4, purity ≥99.0%) were procured from Sigma–Aldrich, Germany. Trisodium citrate dihydrate (TSC) ($Na_3C_6H_5O_7 \bullet 2H_2O$, purity >99.0%) was obtained from Johnson Matthey Co. Ltd., U.K. The DNA sequences used in the preparation of conjugates are listed in Table 1, and were acquired from Integrated DNA Technologies, USA. These DNA sequences were modified with a thiol linker at the 3′-terminus and with ATTO 633 (a red wavelength fluorescence dye) at the 5′-terminus.

2.5.2. Synthesis of AuNPs Colloidal Suspension

The colloidal suspension of AuNPs was prepared using a variant of the Turkevich method[25] in a 250 mL round bottom flask. Initially, 93 mL of water was added to the flask and heated. To prevent contamination and water evaporation during synthesis, an aluminum foil was used to cover the flask. Once the water reached the boiling point, 5 mL of 10 mM AuCl3 aqueous solution was added to the flask, and after 2 min interval, 2 mL of 100 mM TSC aqueous solution was introduced within 5 s. The reaction was allowed to proceed for 15 min before quenching in a water bath at room temperature. The red colloidal suspension products indicated the presence of dispersed 13 nm diameter, citrate-capped AuNPs in water.

2.5.3. Freeze-Thaw Method for the Preparation of AuNPs-DNA Conjugates

Both the DNA sequences as listed in Table 1 were conjugated with the AuNPs by the method of freeze thawing.[28–31] For the synthesis, first 30 µL of DNA sequence were introduced into 1 mL of the AuNPs colloidal suspension placed in centrifuge tubes, where a half-concentration of the colloidal suspension was used. The samples were stored in a freezer for 3 h at −20 °C and subsequently thawed at room temperature for 30 min. Following the formation of AuNPs-DNA conjugates, the samples were centrifuged (13 000 rpm, 15 min) and washed 3 times, to remove unbound DNA using 25 mM potassium phosphate buffer (KPP, pH

7.0). The obtained conjugates were dispersed in the KPP buffer for further analysis.

2.6. Measurement Setup

The AuNPs-DNA conjugate solution was placed in a cuvette in line with the optical light path and heated with 5 °C steps. At each step, parallel spectral and temperature measurements were made with the two AFEs of the portable readout system. For the fluorescence measurements carried out in this work, an optical filter was placed in the optical path of the spectrometer with a center wavelength of 660 ± 5 nm and an optical density of ≥4.0 (Unit 1, Edmund Optics Ltd., USA). For heating of the sample, a water-cooled Peltier thermostat was used. For the temperature-dependent measurements, the RTD PT1000 was placed on the heating cell close to the cuvette and was connected to the temperature AFE module with a four-wire connection. The MAX31865 processed the input from the PT1000 temperature sensor and its ADC output was then converted to the real temperature using Equations (2) and (3). The performance of the mini-spectrometer of the portable system was compared with a desktop instrument (FP-8300, Jasco Inc., USA).

3. Results and Discussion

3.1. Calibration of the Portable Setup

For the calibration of the optical AFE of the portable system, we used a Jasco FP-8300 fluorescence spectrometer in the configuration as schematically shown in **Figure 3**. Since we did not implement a light source in the portable system yet, we combined the light source of the FP-8300 spectrometer with the portable readout system as shown in Figure 3a. For the optical measurements, the excitation wavelength was set to 625 ± 5 nm in the FP-8300 spectrometer. The light source of this instrument is very precise. Therefore, we were just comparing the quality and preciseness of the detection unit. For the reference measurement shown here, the AuNPs-DNA (QP-DNA1) conjugate was used at 75 °C. In Figure 3b in the lower graph, the result of a direct measurement of the desktop spectrometer is shown. A large excitation peak at 625 nm and a small detection peak for the fluorescence light at ≈657 nm can be seen. In our assay with the AuNP-DNA conjugates, however, we were only interested in the FRET effect visible at 657 nm. Therefore, we placed a filter in the optical path of the mini-spectrometer of the portable instrument, which blocked a significant amount of light in the excitation wavelength. As it can be seen in Figure 3b top and middle, this blocking was not complete but significant. By this, we were able to use the internal amplification of the C12880MA mini-spectrometer to visualize the small effects of the thermal expansion of the DNA quadruplexes at the AuNPs. In order to amplify the output of the C12880MA mini spectrometer, we set the exposure time of the CMOS linear image sensor to 75 milliseconds. Of course, we could also install such a filter in the light path of the Jasco FP-8300 spectrometer, which would result in a similar effect. This, however, is not to typical configuration of this instrument.

Using the filter and the internal amplification of the C12880MA mini-spectrometer resulted in a higher intensity at

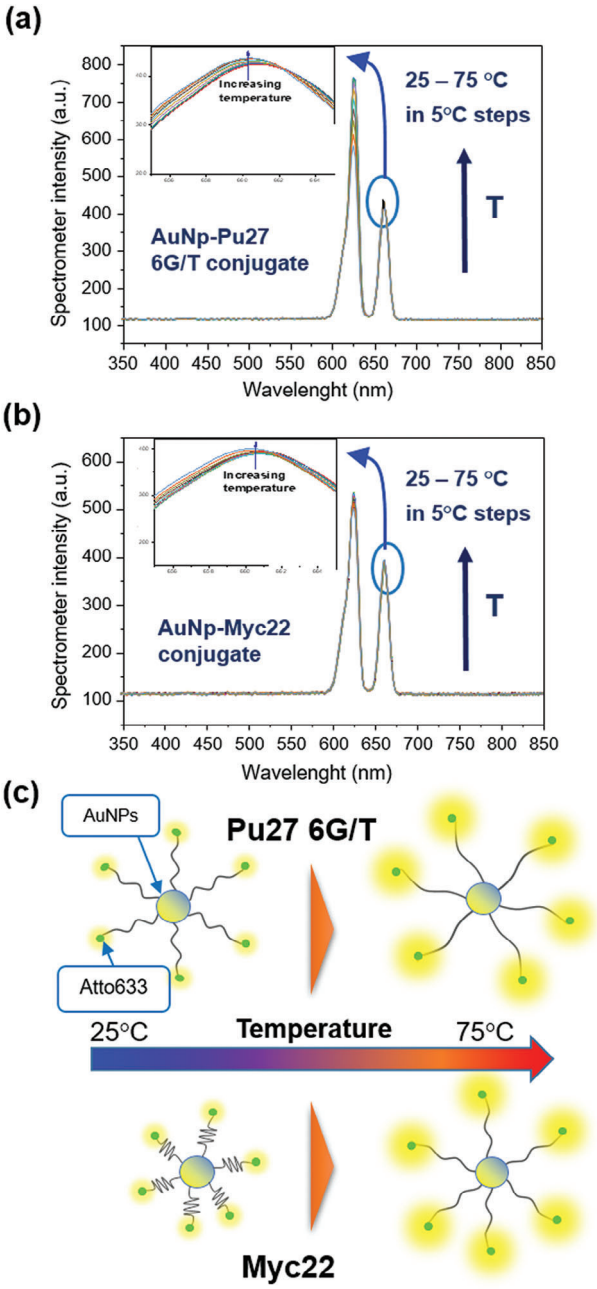

Figure 4. Optical spectra of the two different AuNPs – G-quadruplex DNA conjugates. a) AuNPs – Pu27 6G/T and b) AuNPs – Myc22 conjugates recorded by the optical AFE module of the portable system with varying temperatures from 25 to 75 in 5 °C steps. The excitation wavelength of the light source from the desktop spectrometer was set to 625 ± 5 nm. The peak centered at 625 nm stems from the non-perfect blocking of the filter in the optical path. The peak centered at 660 nm reflects the fluorescence response. c) Sensor principle to detect the unfolding of G-quadruplex DNA using a FRET-based mechanism. Left: In the folded form of the G-quadruplex DNA, the fluorophore is in close vicinity to the AuNP, which leads to quenching of the fluorescence. Right: Once the temperature is increased, the G-quadruplex DNA unfolds and elongates, which leads to a recovery of the fluorescence.

the emission wavelength of 657 nm as compared to the FP-8300. The relative peak intensities (excitation and emission) of both optical spectra captured from portable readout system and the desktop spectrometer were comparable with a peak difference of less than 1 nm (Figure 3b). For the temperature sensor AFE module consisting of PT1000 and MAX31865, the recorded temperature was within 0.5 °C margin of the total accuracy overall operating conditions as stated in the datasheet.

3.2. Temperature-Dependent FRET-Based Fluorescence Recovery Measured with the Portable Setup

The optical spectra recorded with increasing temperature are plotted in **Figure** 4a,b. Two peaks can be seen. The larger peak at 625 nm stems from the excitation light, which is only partly blocked by the optical filter with an optical density of 4.0. The fluorescence intensity of both AuNP-DNA conjugate sequences at ≈657 nm increased with temperature. This can be explained by an extension of the DNA sequences with increasing temperature, which resulted in an increasing distance between the fluorophore dye from the NPs, thereby reducing the FRET-based fluorescence quenching effect as illustrated in Figure 4c.

To elucidate this effect closer, we extracted the differences in the absolute fluorescence intensities at 657 nm for both AuNP-conjugates and plotted them against the recorded temperature as shown in **Figure** 5. In the temperature-dependent graphs, we can clearly observe a different unfolding behavior of both Au-NP-DNA conjugates as expected from their base pair sequences. With increasing temperature, in both cases the fluorescence intensity increases. In case of the Pu27 6G/T AuNP-DNA conjugate after a plateau from 25 to 40 °C a linear increase of the fluorescence can be seen. In the case of the Mcy22 AuNP-DNA conjugate the fluorescence intensity also increases in total, but a lower fluorescence is observed at temperatures ≈40 °C (Figure 5).

Due to the quadruplex nature of the Mcy22 AuNP-DNA conjugate, a different unfolding behavior is indeed expected. In the temperature range between 35 and 45 °C, the FRET-based quenching effect is eventually increased hinting toward an even closer proximity between the fluorophore and the AuNPs. However, to elaborate this effect more precisely, we would need further investigations with reference methods, which is beyond the scope of this work. Here with our modular multi-parametric and portable readout system we demonstrate with this assay, that precise optical spectra and temperature recordings are possible in parallel. The temperature measured with the AFE module was proportional to the temperature set by the FP-8300 spectrometer, but ≈0.15 –0.20 °C lower. This is because the Pt1000 RTD was connected to the body of the heating cell with eventually a weaker thermal contact. The set and recorded temperatures of the AFE module are summarized in **Table** 2. In addition, the emission peaks show a small hypsochromic shift for both the AuNP-DNA conjugates of about a nanometer with the increase of temperature. This is attributed to the gradual unfolding of the sequences and ensuing conformational changes of AuNP-DNA conjugates. Such hypsochromic shifts manifested above 60 °C for AuNPs modified with Myc-22 suggesting the fluorophore remaining near NP surface at lower temperatures. Stable fluorescence signal for AuNPs modified with Myc-22 at lower temperatures

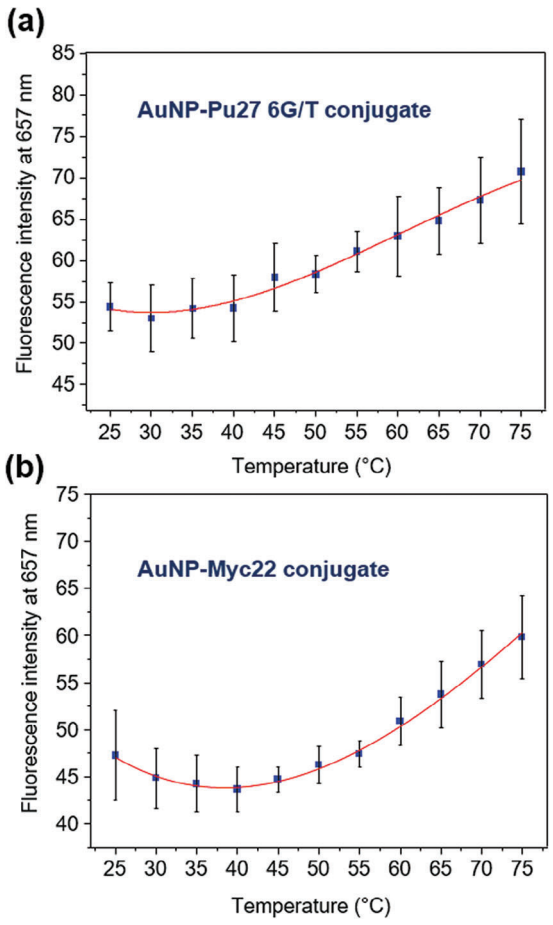

Figure 5. Absolute fluorescence intensity (a.u.) of the two different AuNP-DNA conjugates. The intensities for the a) Pu27 6G/T and b) Myc22 conjugates versus temperature are shown (n = 3 experiments, mean ± standard deviation). It can be seen that temperature and optical response can be monitored by the portable readout system.

also corroborate temperature related effects, as can be seen in Figure 5b. Langer et al. reported a similar hypsochromic shift of the Cy5 upon conformational change (duplex formation) of a DNA sequence.[32]

4. Conclusion and Outlook

We developed a portable, battery-powered, and multi-purpose readout system for parallel optical and thermal measurements of material samples in liquid phase. The system design followed an open-ended approach with four customizable analog frontend inputs. We implemented in the current version two different analog inputs with a highly sensitive optical mini-spectrometer and a precise thermal recording circuit. The optical frontend modules of the portable system were calibrated with a desktop fluorescence spectrometer. An optical filter in the light path of the portable mini-spectrometer allowed for post-amplification of the fluorescence light detection. As a proof-of-concept we selected a FRET-based assay using two different AuNPs-DNA conjugate sequences, which are known to unfold with rising temperature. The fluorescence intensity of two AuNPs-DNA conjugates was

Table 2. Comparison of the temperature recorded by the temperature sensor AFE with respect to the set temperature by FP-8300.

Set Temperature [°C]	ADC output	Temperature [°C]
25	8939	24.81
30	9098	29.85
35	9258	34.92
40	9412	39.80
45	9570	44.83
50	9729	49.89
55	9886	54.89
60	10040	59.81
65	10194	64.86
70	10356	69.92
75	10508	74.80

measured while setting and recording the temperature precisely. For both DNA sequences, a temperature-dependent fluorescence increase based on the FRET mechanism was observed. Due to the distinct structure of the two sequences, a difference in the unfolding mechanism was observed but would need further investigation to confirm these results. The temperature range for the FRET-based fluorescence recovery measurements was kept in between 25 and 75 °C. An increase in temperature above 75 °C is expected to saturate the fluorescence signal. We have seen that a saturation happens ≈85 °C for our AuNPs-DNA conjugates, but this is strictly avoided due to non-reversibility conditions for the FRET mechanism.

The portable, battery-powered, multi-purpose readout system presented here is, however, not limited to synchronous optical and thermal measurements. The modular design and the open-ended feature of the readout system will enable a quick adaptation of other measurements methods, assay or techniques. For example, the remaining channels of the main board could be utilized to read the input of ion-sensitive field-effect transistors (ISFET) as pH-sensitive sensors or offer a current measurement scheme for amperometric sensing of chemical or biological species. There also two channels that could be equipped with the same AFE module to measure heat flow from one area to the other or to measure two ISFET in a differential mode. Based on the planned chemical or biological sensor assay, other AFE modules could be designed and implemented to meet the measurement requirements. There the main advantage is the parallel recording and data logging. This will allow for future combinatorial assays using complementary transducer principles along with machine learning-based data analysis for robustness against adverse influences of interfering side-parameters. In this present work, the light source form FP-8300 spectrometer was utilized, but the optical AFE module has an option for incorporating additional LED, which can be installed in the future based on the requirement of the assay and measurement technique.

Acknowledgements

This work was supported by the Interreg Euregion Meuse-Rhine, project "Food Screening EMR" (EMR159), funded by the European Regional Development Fund of the European Union. We also thank the Advanced Research Opportunities Program (AROP) of RWTH Aachen University for supporting Thossaporn Wijakmatee during this exchange project in IWE 1. Additional support came from the "Exploratory Research Space" (ERS) program of RWTH Aachen University under the project G4-NeuroTec (OPSF581).

Conflict of Interest

The authors declare no conflict of interest.

Data Availability Statement

The data that support the findings of this study are available from the corresponding author upon reasonable request.

Keywords

DNA, fluorescence spectroscopy, FRET, gold nanoparticles, optical spectroscopy, point-of-care, portable readout system

Received: July 11, 2024
Revised: September 6, 2024
Published online: October 7, 2024

[1] J. P. Gosling, *Enzyme Immunoassay. In Immunoassay*, (Eds: E. P. Diamandis, T. K. Christopoulos), Academic Press, San Diego **1996**, pp 287.
[2] K. Abels, E. M. Salvo-Halloran, D. White, M. Ali, N. R. Agarwal, V. Leung, M. Ali, M. Sidawi, A. Capretta, J. D. Brennan, J. Nease, C. D. M. Filipe, *ACS Omega.* **2021**, *6*, 22439.
[3] V. A. Lemos, A. L. de Carvalho, *Environ. Monit. Assess.* **2010**, *171*, 255.
[4] G. L. Ellman, K. D. Courtney, V. Andres, R. M. Featherstone, *Biochem. Pharmacol.* **1961**, *7*, 88.
[5] S. L. Ullo, G. R. Sinha, *Sensors* **2020**, *20*, 3113.
[6] M. Szczerska, P. Wityk, P. Listewnik, *J. Biophotonics.* **2023**, *16*, e202200186.
[7] H. F. Arata, P. Löw, K. Ishizuka, C. Bergaud, B. Kim, H. Noji, H. Fujita, *Sens. Actuators, B* **2006**, *117*, 339.
[8] A. E. Oliver, G. A. Baker, R. D. Fugate, F. Tablin, J. H. Crowe, *Biophys. J.* **2000**, *78*, 2116.
[9] S. Pistolesi, N. Tjandra, *Biochemistry* **2012**, *51*, 643.
[10] A. R. Shafiqa, A. A. Aziz, B. Mehrdel, *J. Phys: Conf. Ser.* **2018**, *1083*, 012040.
[11] M. A. M. Duque, N. Rhowell, J. Tiozon, R. C. N. España, *bioRxiv* **2016**, 044875, https://doi.org/10.1101/044875.
[12] C. Rodríguez Díaz, N. Lafuente-Gómez, C. Coutinho, D. Pardo, H. Alarcón-Iniesta, M. López-Valls, R. Coloma, P. Milán-Rois, M. Domenech, M. Abreu, R. Cantón, J. C. Galán, R. Bocanegra, L. A. Campos, R. Miranda, M. Castellanos, Á. Somoza, *Talanta* **2022**, *243*, 123393.
[13] B. Li, X. Li, Y. Dong, B. Wang, D. Li, Y. Shi, Y. Wu, *Anal. Chem.* **2017**, *89*, 10639.
[14] J. Zhang, L. Wang, D. Pan, S. Song, F. Y. C. Boey, H. Zhang, C. Fan, *Small* **2008**, *4*, 1196.
[15] H. Ueyama, M. Takagi, S. Takenaka, *J. Am. Chem. Soc.* **2002**, *124*, 14286.
[16] T. Li, E. Wang, S. Dong, *Anal. Chem.* **2010**, *82*, 1515.
[17] H. Wei, B. Li, J. Li, S. Dong, E. Wang, *Nanotechnology* **2008**, *19*, 095501.

[18] E. Dulkeith, A. C. Morteani, T. Niedereichholz, T. A. Klar, J. Feldmann, S. A. Levi, F. C. J. M. van Veggel, D. N. Reinhoudt, M. Möller, D. I. Gittins, *Phys. Rev. Lett.* **2002**, *89*, 203002.
[19] N. Kosiol, S. Juranek, P. Brossart, A. Heine, K. Paeschke, *Mol. Cancer.* **2021**, *20*, 40.
[20] S. Chuaychob, C. Thammakhet-Buranachai, P. Kanatharana, P. Thavarungkul, C. Buranachai, M. Fujita, M. Maeda, *Anal. Methods.* **2020**, *12*, 230.
[21] C. M. Olsen, L. A. Marky, In *G-Quadruplex DNA: Methods and Protocols*, (Ed: P. Baumann), Humana Press, Totowa, NJ **2010**, pp. 147.
[22] O. R. Molnár, A. Végh, J. Somkuti, L. Smeller, *Sci Rep-Uk* **2021**, *11*, 23243.
[23] J. Y. Lee, B. Okumus, D. S. Kim, T. Ha, *Proc. Natl. Acad. Sci. USA* **2005**, *102*, 18938.
[24] A. De Cian, L. Guittat, M. Kaiser, B. Saccà, S. Amrane, A. Bourdoncle, P. Alberti, M.-P. Teulade-Fichou, L. Lacroix, J.-L. Mergny, *Methods* **2007**, *42*, 183.
[25] LattePanda LattePanda 3 Delta. https://www.lattepanda.com/lattepanda-3-delta (accessed July 2024).
[26] V. Rauser, E. Weinhold, *ChemBioChem.* **2020**, *21* 2445.
[27] S. Burge, G. N. Parkinson, P. Hazel, A. K. Todd, S. Neidle, *Nucleic. Acids. Res.* **2006**, *34*, 5402.
[28] B. Liu, T. Wu, Z. Huang, Y. Liu, J. Liu, *Angew. Chem., Int. Ed.* **2019**, *58*, 2109.
[29] B. Liu, J. Liu, *Langmuir* **2019**, *35*, 6476.
[30] X. Zhang, M. R. Servos, J. Liu, *J. Am. Chem. Soc.* **2012**, *134*, 7266.
[31] B. Liu, J. Liu, *Anal. Methods.* **2017**, *9*, 2633.
[32] A. Langer, T. Bartoschik, O. Cehlar, S. Duhr, P. Baaske, W. Streicher, *Assay. Drug. Dev. Technol.* **2022**, *20*, 83.